THE JOURNAL OF PHYSICAL CHEMISTRY A

© Copyright 2001 by the American Chemical Society VOLUME 105, NUMBER 25, JUNE 28, 2001

LETTERS

Simultaneous Determination of Structural and Kinetic Parameters Characterizing the Interconversion of Highly Dispersed Species: the Interaction of NO with $Rh^I(CO)_2/\gamma$-Al_2O_3

Mark A. Newton,*,† Daryl G. Burnaby,† Andrew J. Dent,‡ Sofia Diaz-Moreno,§ John Evans,*,† Steven G. Fiddy,† Thomas Neisius,§ Sakura Pascarelli,§ and Sandra Turin†

Department of Chemistry, University of Southampton, Highfield, Southampton, U.K. SO17 1BJ, European Synchrotron Radiation Facility, Grenoble, France, and CLRC Daresbury, Warrington, UK, WA4 4AD

Received: April 27, 2001

Energy-dispersive EXAFS (EDE), combined with mass spectrometry and a flow microreactor system, has been used to investigate the reaction of an Al_2O_3-supported $Rh^I(CO)_2$ species with NO. This combined in situ approach uniquely permits a priori analysis of the structures of the species involved (on a time scale of ca. 2 s) and simultaneous determination of reaction mechanism and kinetic parameters. In the current case, it is found that the $Al(O)Rh^I(CO)_2Cl$ species reacts to form an intermediate $Al(O)Rh(NO)_2Cl$ Cl species ($\nu \approx 0.357 \pm 0.125$ s^{-1}, $E_{act} \approx 11 \pm 1.25$ kJ mol^{-1}), which subsequently forms an $(AlO)_2Rh(NO)^-Cl$ species and $N_2O_{(g)}$ ($\nu \approx 2 \pm 0.5 \times 10^4$ s^{-1}, $E_{act} \approx 40 \pm 3.5$ kJ mol^{-1}) showing a bent (134°) RhNO bond. This combination of rapid and complementary techniques should be applicable to a wide range of disciplines where quantitative structural and kinetic determinations are of importance.

Delineating the relationships between structure and the reactivity is a common goal in many areas of science. In catalysis, such determinations are pivotal to understanding of how a given catalyst works and, therefore, how one may design or modify a catalyst for a specific purpose. A true understanding of such relationships may only be gained through the application of experimental probes that allow in situ determination of molecular structure with simultaneous exploration of how particular species interact with their environment. By combining energy-dispersive EXAFS (EDE) with a flow microreactor and mass spectrometry, we show that reactions between surface bound, catalytically relevant species can be followed on a time scale of seconds in a way that allows a priori structural determination of the species involved. We determine the structure of the surface bound nitrosyl species formed from the interaction of NO with a supported $Rh^I(CO)_2$ species. Further, we show how this approach yields information regarding the mechanism of reaction and the kinetic parameters that characterize individual steps in a reaction sequence.

Time-resolved EXAFS methodologies have begun to allow EXAFS to be applied in determining local order change during chemical reactions.[1−10] Quick EXAFS (QEXAFS),[1,5−8] wherein the stepwise progression of the monochromator through a particular energy window is optimized, has been widely developed and commonly allows EXAFS spectra to be taken in ∼30−60 s. Though faster experiments have been reported,[5] the range of data obtained only permits analysis of changes in the near edge structure. Subsequently structural information may only be implied through reference to known standards.

Energy-dispersive EXAFS (EDE)[2−4,9,10] eliminates all monochromator movement by using an elliptically bent monochromator to illuminate the sample with a window of X-ray energies

* Corresponding authors. M.A.N.: e-mail, m.a.newton@soton.ac.uk; tel, + 44 (0)2380 596744. J.E.: e-mail, je@soton.ac.uk; tel, +44 (0)2380 593307; FAX, +44 (0)2380 593781.
† University of Southampton.
‡ CLRC Daresbury.
§ European Synchrotron Radiation Facility.

10.1021/jp011621x CCC: $20.00 © 2001 American Chemical Society
Published on Web 05/31/2001

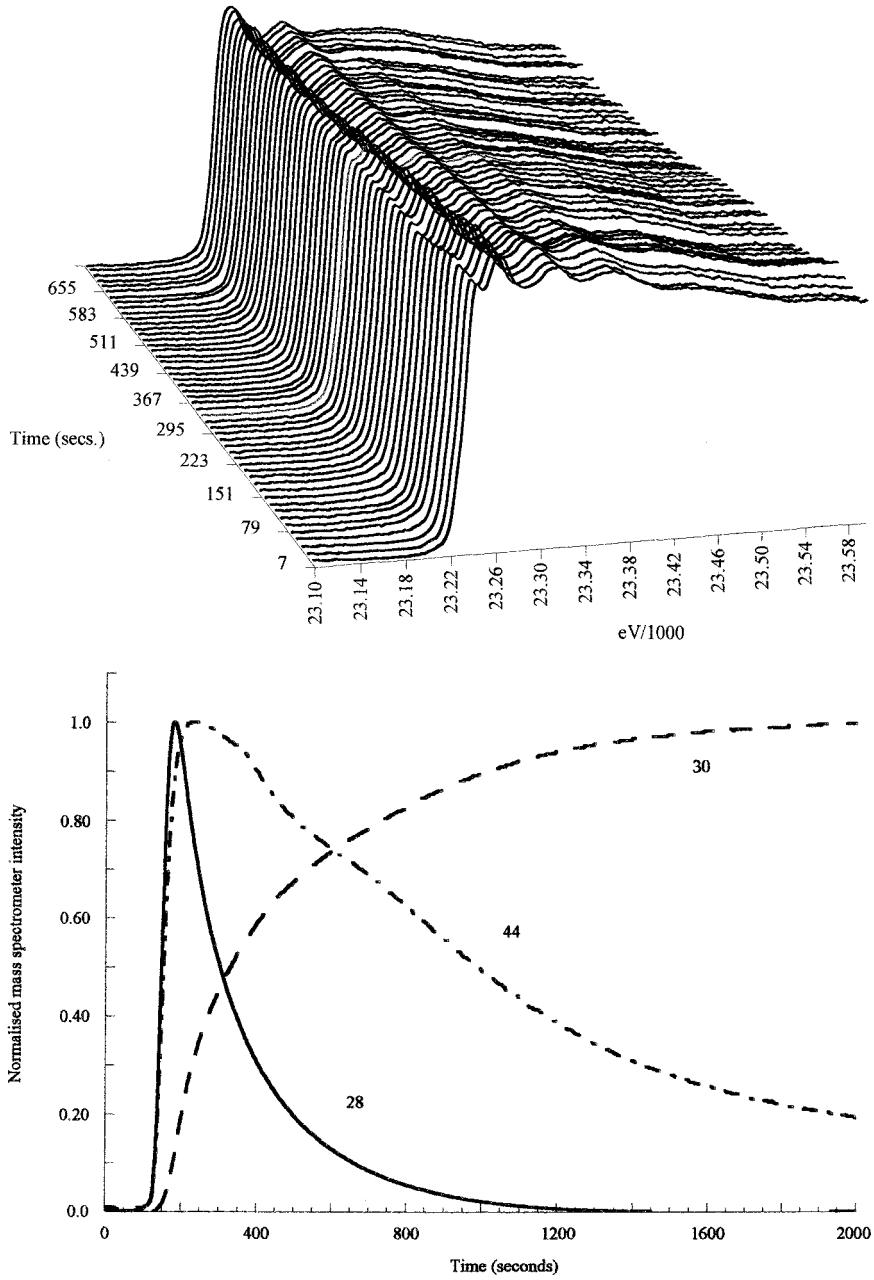

Figure 1. (a) Rh *k*-edge EDE spectra obtained during the reaction of $Rh(CO)_2Cl/Al_2O_3$ with 5 mL min^{-1} NO (5%) in He at 338 K. Each spectrum has a total acquisition time of ∼1.95 s (100 scans/spectrum, 1.3 ms/scan, 15 "stripes"). For clarity, alternate spectra only are shown. (b) Normalized mass spectrometer traces obtained during the reaction of $Rh(CO)_2Cl/Al_2O_3$ with 5 mL min^{-1} NO (5%) in He at 308 K. The masses corresponding to each trace are indicated.

and the potential for extremely fast data collection; it is, however, demanding in terms of sample presentation. This has meant that since the first applications of EDE to heterogeneous systems,[2−4] subsequent studies[9,10] have been limited to pressed disk samples, which may pose problems with sample degradation and gas permeability.[11] In general, detailed structural information has not been forthcoming, though correlations between catalytic activity and changes in catalyst phase have been amply demonstrated.

We have recently shown that EDE of the quality required for detailed structural analysis can be derived from powder samples, maintained in a tube reactor, on a time scale of seconds.[12] This approach has now been extended to simultaneous mass spectrometric determination of reactant uptake and product evolution during the course of a reaction (that between a supported $Rh^I(CO)_2$ and NO). Here we discuss the formation of the nitrosyl adduct; a more detailed discussion of the reverse reaction will be given elsewhere.[13]

Al_2O_3 was heated in Ar at 493 K for 6 h. $[Rh(CO)_2Cl]_2$ was subsequently sublimed under vacuum onto dried, hydroxylated Al_2O_3 to a loading of ∼5 wt % Rh. The resulting yellow powder was kept under an inert atmosphere before use. Ten milligrams of supported sample was packed in a quartz tube (∼3 mm i.d, 0.2 mm wall thickness, ∼5 mm bed length) and loaded into a cell described previously.[12] CO was passed over the sample, which was then flushed with He before switching feed to 2.5% NO/He (5 mL/min).

EDE measurements were made on beamline ID24 at the ESRF, using an asymmetrically cut (6°) Si(111) monochromator in Laue configuration.[8] A masked, peltier-cooled CCD detector (Princeton) was used to collect the EDEXAFS data, with 18 spectra (of which 10 were summed to a single aquisition) being

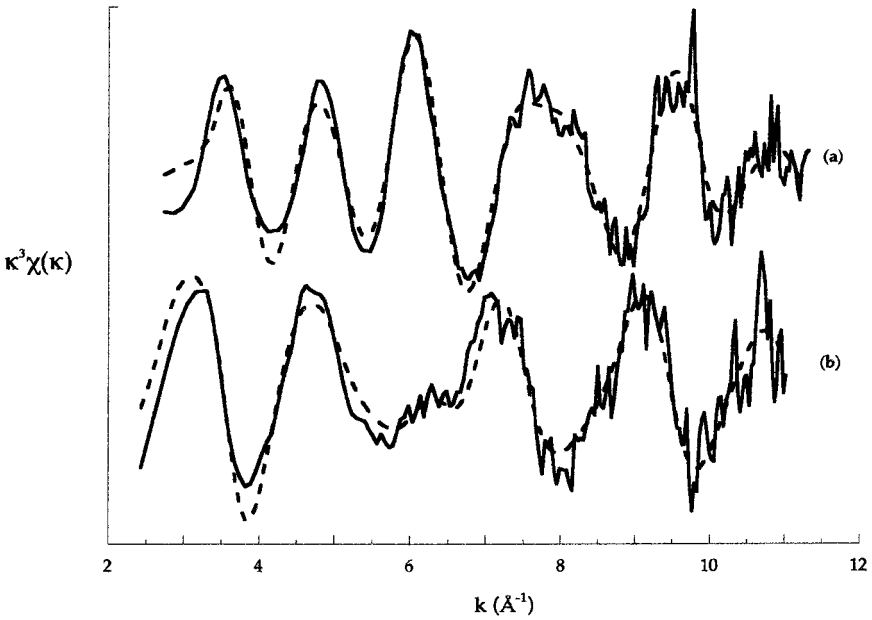

Figure 2. k^3-weighted EDE spectra for the $Rh(CO)_2Cl/Al_2O_3$ sample (a) and that derived after exposure to NO (data collection times as Figure 1a). In each case, the solid line is the experimental data, and the dashed line is the best fit derived from EXAFS analysis in EXCURVE 98.

TABLE 1: Best Fit Structural and Statistical Parameters Derived from Explicit Analysis (in EXCURVE 98[14b]) of the EXAFS Data Shown in Figure 2[a]

	geminal dicarbonyl			Rh nitrosyl	
scatterer	distance from Rh (Å)	$2s^2/Å^2$	scatterer	distance from Rh (Å)	$2\sigma^2/Å^2$
C1 (carbonyl)	1.850 (1.853 ± 0.026)	0.003	N	2.007 (1.98 ± 0.069)	0.003
C2 (carbonyl)	1.925 (1.893 ± 0.030)	0.001	O1 (nitrosyl)	2.842 (2.815 ± 0.054)	0.013
Cl	2.383 (2.366 ± 0.029)	0.001	Cl	2.417 (2.40 ± 0.052)	0.001
O1 (carbonyl)	2.968 (2.989 ± 0.033)	0.01	O2(Al)	2.106 (2.106 ± 0.049)	0.008
O2 (carbonyl)	3.075 (3.033 ± 0.035)	0.014	O3(Al)	2.008 (1.985 ± 0.040)	0.002
O3 (Al)	2.155 (2.165 ± 0.040)	0.014	Al1	3.604 (3.59 ± 0.061)	0.002
Al	3.691 (3.662 ± 0.040)	0.031	Al2	3.707 (3.72 ± 0.034)	0.010
	R factor	33.72		*R* factor	45.26

[a] Also shown (in parentheses) are average parameters and standard deviations obtained from 15 independent measurements and analyses.

collected prior to readout. Data reduction was carried out using PAXAS[14a] and spherical wave analysis using EXCURVE 98.[14b]

The reactor was connected to a Balzers mass spectrometer allowing16 masses to be followed simultaneously. Effluent gas from the cell passed through a packed silica capillary before entering the turbo molecular pumped mass spectrometer via a differentially pumped flange.

Figure 1a shows Rh K-edge EDE data for the exposure of $Rh^I(CO)_2/Al_2O_3$; Figure 1b shows the corresponding mass spectrometer traces for NO, CO, and mass 44. Each spectrum has a total acquisition time of ~1.95 s, but the repetition rate is limited by detector readout: in this case, one spectrum is taken every 7.2 s. As NO passes through the bed, CO is evolved followed by the slower appearance of mass 44. At the same time, the characteristic EXAFS signature of the $Rh^I(CO)_2$ species is replaced with a new spectrum.

Figure 2 shows k^3-weighted EDE (and the corresponding theoretical EXAFS) derived from (a) the starting $Rh^I(CO)_2$ system and (b) the final NO adduct; the corresponding structural and statistical parameters derived from the fitting of the data are shown in Table 1, and the numbers in parentheses are 15 derived independent measurements and are presented as an estimate of the errors associated with each determination.[24]

Analysis shows that the Rh−Cl coordination is retained and that no Rh−Rh coordination is apparent. An inequivalence of the CO groups in the geminal species (due to a trans influence of the Cl vs the O(Al) linkage) is also suggested, though the difference in bond lengths falls just outside the error associated with our measurements.

The final product of the reaction is best modeled as a monodisperse, square planar species containing a single NO ligand in a bent (~134°) configuration, the reduction in the multiple scattering contribution to the $RhO^{(NO)}$ shell indicating a strongly bent nitrosyl ligand. This assignment is confirmed by diffuse reflectance infrared spectroscopy, with the chracteristic carbonyl spectrum due to the geminal dicarbonyl species ($\nu_{sym}(CO) \approx 2110\ cm^{-1}$, $\nu_{assym}(CO) \approx 2030\ cm^{-1}$) being replaced by a nitrosyl band at $\sim 1750\ cm^{-1}$,[13] consistent with the "bent" nature of the Rh(NO) bond in the reaction product.[16]

The nitrosyl shows two distinct (in terms of errors) Rh−O bond attributed to a trans influence, the longer Rh−O distance being derived from the Rh−O bond opposite the NO ligand. The obtained bond lengths (Rh−N and Rh−Cl) are in close agreement with crystallographic determinations of the structures of bent Rh−NO species such as $Rh(O_2CCF_3)_2(NO)(PPh_3)$[15a] and $RhCl_2(NO)(PPh)_3)_2$.[15b] The net conversion is therefore

$$Al(O)\text{-}Rh(CO)_2Cl \rightleftharpoons [Al(O)]_2Rh(NO)^-Cl \qquad (1)$$

It can be shown that each of the spectra in Figure 1a can be expressed as an appropriately weighted combination of the starting and end spectra. Figure 3 shows a plot of the normalized intensities of an EXAFS (~23375 eV, present only in the

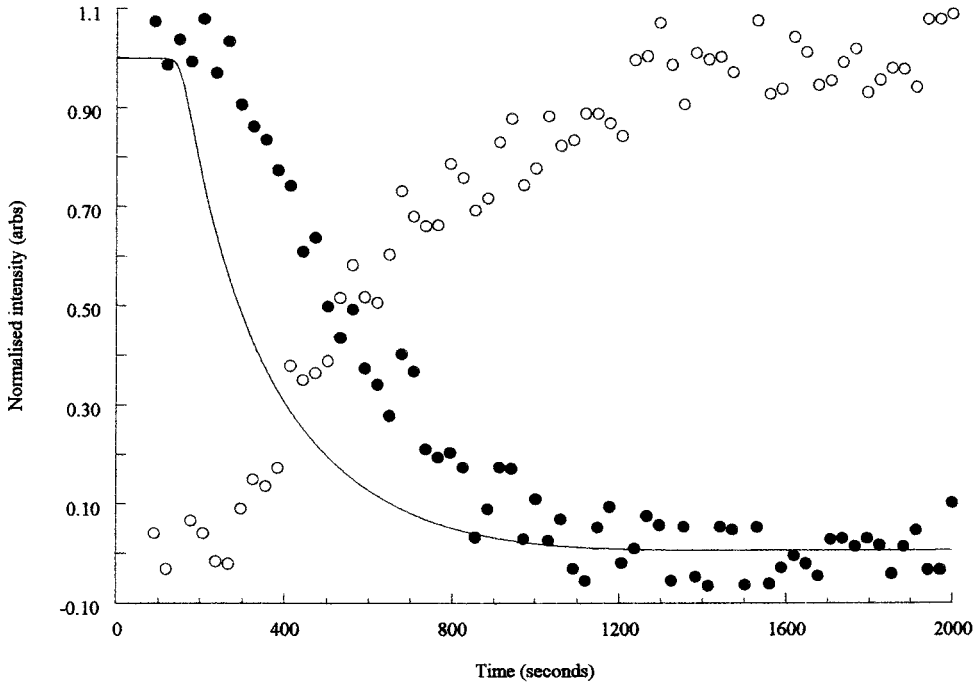

Figure 3. Temporal variation in the intensity of XANES (open circles) and EXAFS (filled circles) features and CO evolution during exposure of $Rh(CO)_2Cl/Al_2O_3$ to NO at 308 K. The EXAFS intensities have been normalized to a starting concentration of 1. The CO data is shown in the following form: [(1 − (integral CO vs time))/(total CO evolved)].

starting spectra) and an XANES feature (~23260 eV, indicative of the product), alongside CO evolution data, as a function of time.

It is clear that the release of CO from the sample and the changes in the EXAFS spectra occur on differing time scales, indicating two discrete reaction stages.

The first stage involves the release of CO with little or no change in the observed EXAFS. The initial reaction of the $Rh^I(CO)_2Cl$ therefore results in a species that, in terms of the local Rh coordination sphere, is very similar. By inference, the reaction proceeds via an intermediate species that is either Rh-(CO)(NO)Cl or $Rh(NO)_2Cl$. The only previous determination of structure for an inorganic Rh species of either type ($[Rh(NO)_2(PPh_3)_2][ClO_4]$[17]) displays Rh−N bond lengths only 0.03 Å shorter than that indicated for the $Rh(CO)_2Cl$ species from our analysis with an RhNO bond angle of ~159°. A priori, as this intermediate species will be present in relatively low transient concentrations coexisting with remaining $Rh(CO)_2Cl$ species, EDE alone will not allow us to determine which species predominates.

However, comparison of the total amount of CO released in this mass spectral trace with CO consumed by the reverse reaction[13] shows that all the CO ligands present in the $Rh^I(CO)_2Cl$ adlayer are released to the gas phase in this single (mass spectral) event. It therefore seems that the initial product of this reaction is $Al(O)Rh(NO)_2Cl$.

The implied reaction mechanism is therefore

$$2NO_g + Al(O)\text{-}Rh(CO)_2Cl \overset{k_1}{\Longrightarrow} Al(O)\text{-}Rh(NO)_2Cl + 2CO_g \quad (2)$$

$$Al(O)\text{-}Rh(NO)_2Cl \overset{k_2}{\Longrightarrow} Al(O)\text{-}Rh(O)(*)Cl + N_2O_g \quad (3)$$

$$NO + Al(O)\text{-}Rh(O)*Cl \overset{k_3}{\Longrightarrow} [Al(O)]_2\text{-}Rh(NO)^-Cl \quad (4)$$

Where (*) represents a free site for NO coordination and step 4 is extremely fast.

Within the above scheme, CO evolution observed in the mass spectrometer yields information regarding eq 2, and the temporal variation of the EDE features reflects the facility of eq 3; it is in this stage that the local coordination sphere changes radically. Figure 4a,b shows mass spectrometric (mass 28) and EDE data (vis a vis Figure 3) for the reaction in the temperature range 293−328 K. Also shown in Figure 4 are the results of applying a simple two-step reaction model for two consecutive first-order reactions[18] and assuming $k_3 \gg k_1$ or k_2, i.e.

$$A \overset{k_1}{\Longrightarrow} B \overset{k_2}{\Longrightarrow} C$$

where

$$[A] = [A]_o e^{-k_1 t}$$

$$[B] = \frac{[A]_o k_1}{k_2 - k_1}(e^{-k_1 t} - e^{-k_2 t})$$

$$[C] = \frac{[A]_o}{k_2 - k_1}[k_2(1 - e^{-k_1 t}) - k_1(1 - e^{-k_2 t})]$$

[A] is the $Rh(CO)_2Cl$ species, [B] is the intermediate $Rh(NO)_2$ adduct, and [C] is the $Rh(NO)^-$ species. The derived activation energies (E_{act}) and pre-exponentials (ν) for steps 2 and 3 of the reaction mechanism are

$$\nu \approx 0.357 \pm 0.125\ s^{-1} \qquad E_{act} \approx 11 \pm 1.25\ kJ\ mol^{-1} \quad (2)$$

and

$$\nu \approx 2 \pm 0.5 \times 10^4\ s^{-1} \qquad E_{act} \approx 40 \pm 3.5\ kJ\ mol^{-1} \quad (3)$$

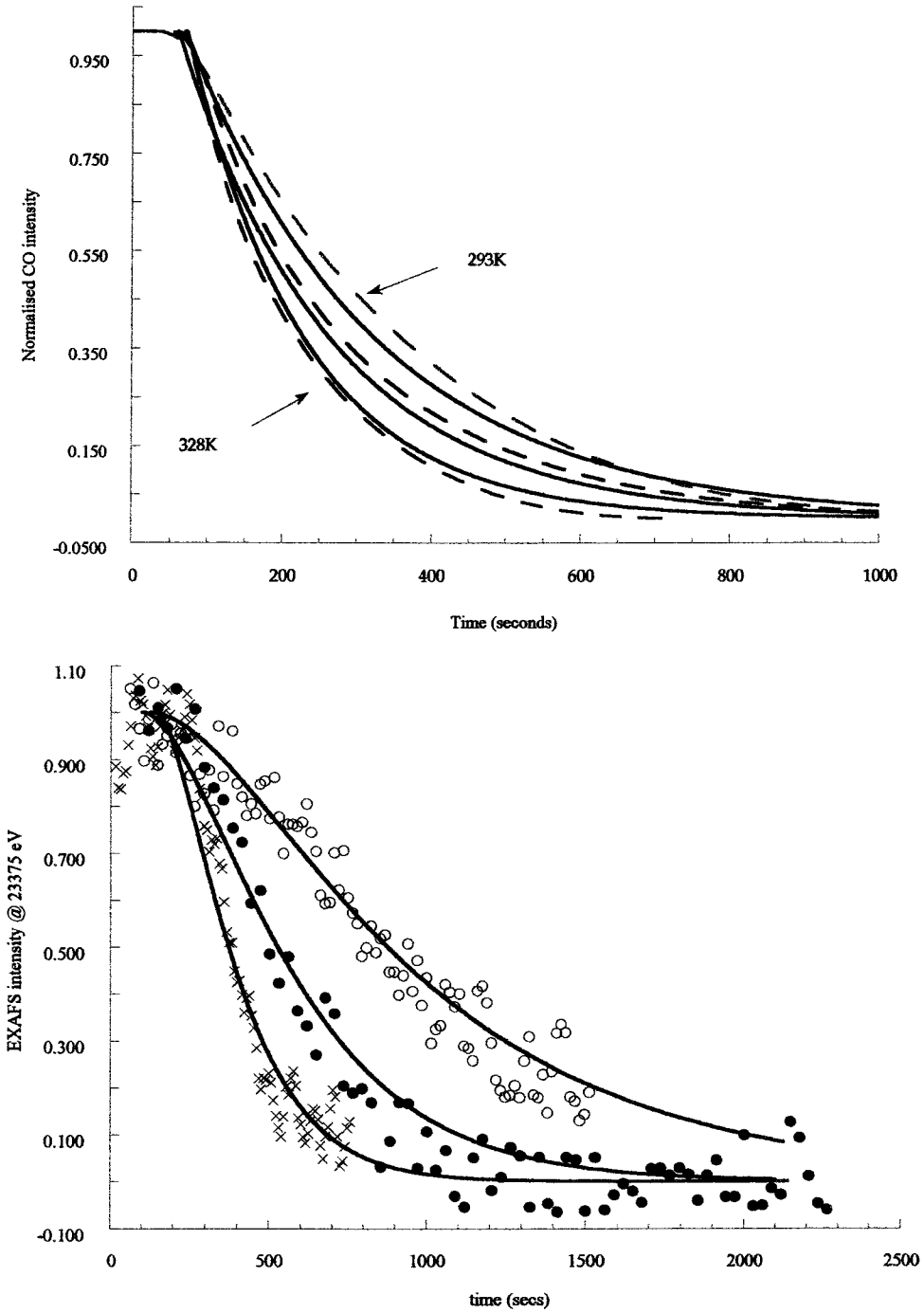

Figure 4. (a) Temporal variation in observed CO evolution during the reaction of $Rh(CO)_2Cl/Al_2O_3$ with NO at three temperatures (293, 308, and 328K). The CO evolution is shown in the same integrated form as that in Figure 3. Alongside the experimental data (hatched lines), fits due to a two-step kinetic model (solid lines; see text) are also shown. The parameters used to describe the CO evolution are $\nu = 0.357 \pm 0.125$ s^{-1} and $E_{act} \approx 11 \pm 1.25$ kJ mol^{-1}. (b) Temporal variation of the EXAFS feature (at 23375 eV) observed to disappear during the reaction of $Rh(CO)_2Cl/Al_2O_3$ with NO at three temperatures (open circles, 293 K; filled circles, 308 K; crosses, 328 K). Also shown (solid line) are fits derived from a two-step reaction model (see text). The kinetic parameters pertaining to this step are $n = 2 \times 10^4$ s^{-1} and $E_{act} \approx 40 \pm 3.5$ kJ mol^{-1} (filled circles).

The parameters derived for step 2 indicate that either the activation energy is due to diffusion of the reactant/product through the bed to the mass spectrometer[19] or this reaction is subject to an extreme steric requirement. The latter would imply that the NO molecules impinging on the surface must do so in a highly specific manner in order to initiate reaction. The magnitude of E_{act} for reaction 2 is consistent with that recently derived for CO exchange processes occurring in $[Rh(CO)_2Cl]_2$.[20] Step 2 can be regarded as analogous to these associative ligand substitution reactions in square planar complexes. In further support of this notion, reaction of $Rh(CO)_2Cl$ supported upon vacuum-reduced TiO_2 shows the same character,[21] as these experiments were made in an ultrahigh vacuum environment diffusion limitations would seem unlikely.

The values obtained for step 3 imply that the rate-determining step for synthesis of the $Rh(NO)^-$ species is an intramolecular reaction. The low pre-exponential most likely indicates that a bond rotation/scissors motion within the geminal is required to achieve the transition state for formation of N_2O. Once formed, the N_2O desorbs, leaving a coordinatively unsaturated Rh center.

This reacts under NO to form the final $Rh(NO)^-$ with the concomitant formation of a second linkage to the oxide surface.

The proposed mechanism is similar to that previously postulated in the homogeneous interaction between the $[RhCl_2(CO)_2]^-$ anion and NO[17], and it is worthy of note that of the various transition metal dinitrosyls active for the production of N_2O from NO and CO Rh systems show the greatest activity.[16] The fate of the O generated in step 3 is not explicitly determinable. H_2O is formed during this reaction,[13] and therefore, we may postulate that this O species scavenges protons from the surface to form H_2O or that it fills surface defects created by the release of H_2O to the gas phase.

Recent work on related systems[22,23] has indeed pointed to supported $Rh(NO)_2$ species also being involved in the production of N_2O. However, this has been surmised to require the presence of Rh^0 species as well as the geminal dinitrosyl. In the current case, as there is no evidence for Rh−Rh interactions, this is not necessarily so, and N_2O may be formed from the unimolecular decomposition of the geminal dinitrosyl itself.

In summary, we have shown that both kinetic and structural data pertaining to chemical transformations occurring in heterogeneous systems can be derived in a truly simultaneous manner and on a time scale of ~2 s through a combination of energy-dispersive EXAFS and mass spectrometry. This methodology has quantified the interactions occurring in what is a relatively simple, yet catalytically relevant, conversion. This approach, though derived for the interrogation of catalyst systems, should be applicable in a number of areas in chemistry, physics, and materials science, where the derivation of structural and kinetic data in situ and at the same time is desirable.

Acknowledgment. This work has been funded under the "Catalysis and Chemical Processes" initiative of the EPSRC and is dedicated to the memory of the late Dr Judith Corker. We would like to thank the ESRF for providing access to the synchrotron. The authors are also extremely grateful to Bruce Hancock, John James, Melanie Hill, Dr. Ralph Wiegel, and Sebastian Pasternak for their technical expertise. Professor R Schlögl is also thanked for the generous provision of the mass spectrometer facility available on ID 24.

References and Notes

(1) See, for instance: (a) Frahm, R. *Nucl. Instrum. Methods A* **1988**, *270*, 588. (b) Dobson, B. R.; Hasnain, S. S.; Neu, M.; Ramsdale, C. A.; Murphy, L. M. *Jpn. J. Appl. Phys.* **1993**, *32*, 192.

(2) Couves, J. W.; Thomas, J. M.; Catlow, R. A. *J. Phys. Chem*. **1990**, *94*, 6517.

(3) Couves, J. W.; Thomas, J. M.; Waller, D.; Jones, R. H.; Dent, A. J.; Derbyshire, G. E.; Greaves, G. N. *Nature* **1991**, *354*, 465.

(4) Sankar, G.; Wright, P. A.; Natarajan, S.; Thomas, J. M.; Greaves, G. N.; Dent, A. J.; Dobson, B. R.; Ramsdale, C. A.; Jones, R. H. *J. Phys. Chem.* **1993**, *97*, 9550.

(5) Clausen, B. S.; Grabaek, L.; Steffensen, G.; Hansen, P. L.; Topsoe, H. *Catal. Lett.* **1998**, *20*, 23.

(6) Cimini, F.; Prins, R. *J. Phys. Chem. B* **1997**, *101*, 5277.

(7) Cattaneo, R.; Weber, T.; Shido, T.; Prins, R. *J. Catal.* **2000**, *191*, 25.

(8) Als Nielsen, J.; Grubel, G.; Clausen, B. S. *Nucl. Instrum. Methods B* **1995**, *97*, 522.

(9) Hagelstein, M.; Ferraro, C.; Hatje, U.; Ressler, T.; Metz, U. *J. Synchrotron Radiat.* **1995**, *2*, 174.

(10) (a) Ressler, T.; Hagelstein, M.; Hatje, U.; Metz, W. *J. Phys. Chem. B* **1997**, *101*, 6680. (b) Ressler, T.; Timpe, O.; Neisius, T.; Find, J.; Mestl, G.; Dieterle, M.; Schlögl, R. *J. Catal.* **2000**, *191*, 75.

(11) See, for instance: Van Der Venne, J. L.; Rindt, J. P. M.; Coenen, G. J. M. M. *J. Colloid Interface Sci*. **1990**, *74*, 287. Conner, W. C.; Weist, E. L.; Ito, T.; Fraissard, J. *J. Phys. Chem.* **1989**, *93*, 4138.

(12) (a) Fiddy, S. G.; Newton, M. A.; Dent, A. J.; Salvini, G.; Corker, J. M.; Turin, S.; Campbell, T.; Evans, J. *Chem. Commun.* **1999**, 851. (b) Fiddy, S. G.; Newton, M. A.; Campbell, T.; Corker, J. M.; Dent, A. J.; Harvey, I.; Salvini, G.; Turin, S.; Evans, J. *Chem. Commun.* **2001**, 445.

(13) Newton, M. A.; Burnaby, D. G.; Dent, A. J.; Diaz-Moreno, S.; Evans, J.; Fiddy, S. G.; Neisius, T.; Turin, S. Manuscript in preparation.

(14) (a) Binsted, N. *PAXAS, Programme for the Analysis of X-ray Absorption Apectra*; University of Southampton: Southampton, U.K., 1988. (b) Binsted, N. *EXCURV98, CCLRC Daresbury Laboratory Computer Programme*; University of Southampton: Southampton, U.K., 1998.

(15) (a) Galas, J. M. R.; Hursthouse, M. B.; Moore, D. S.; Robinson, S. D. *Inorg. Chim. Acta* **1983**, *77*, L135. (b) Goldberg, S. Z.;, Kubiak, C.; Meyer, C. D.; Eisenberg, R. *Inorg. Chem.* **1975**, *14*, 1650.

(16) See, for instance: Eisenberg, R.; Meyer, C. D. *Acc. Chem. Res.* **1975**, *8*, 26.

(17) Kaduk, J. A.; Ibers, J. A. *Inorg. Chem*. **1975**, *14*, 3071.

(18) Laidler, K. J. *Chemical Kinetics*, 10th ed.; McGraw-Hill: New York, 1984.

(19) See, for instance: Satterfield, C. *Heterogeneous Catalysis in Practice*; McGraw Hill Chem. Eng. Series; McGraw-Hill: New York, 1980.

(20) Churlaud, R.; Frey, U.; Metz, F.; Merbach, A. E. *Inorg. Chem*. **2000**, *39*, 304.

(21) Hayden, B. E.; King, A.; Newton, M. A.; Yoshikawa, N. *J. Mol. Catal. A* **2001**, *167*, 33.

(22) See, for instance: Anderson, J. A.; Millar, G. J.; Rochester, C. H. *J. Chem. Soc., Faraday Trans* **1990**, *86*, 571.

(23) Chafik, T.; Kondarides, D. I.; Verykios, X. E. *J. Catal* **2000**, *190*, 446.

(24) The final structural models were calculated using a multiple scattering approach to the molecular cluster. The shells for $Rh^I(CO)_2/Al_2O_3$ were previously identified by scanning EXAFS on the TiO_2 supported analogue. For the nitrosyl product, other models, including linear nitrosyls and $Rh(NO)_2$ species with and without Rh−Cl coordination, were tested. All yielded appreciably higher *R* factors (>10%) than the nitrosyl model presented here.